Enhancement of dielectric properties by optimization of sintering condition in tungsten–bronze structured Ba$_5$SmTi$_3$Nb$_7$O$_{30}$ ferroelectric ceramics

Prasun Ganguly · A. K. Jha · K. L. Deori

Abstract In this work, polycrystalline Ba$_5$SmTi$_3$Nb$_7$O$_{30}$ tungsten–bronze structured ferroelectric ceramics were synthesized by solid-state reaction technique at different sintering temperatures and durations. The X-ray diffractograms reveal the formation of the compounds in orthorhombic crystal system. The density of the compound is observed to increase with increase in sintering temperature and duration. Scanning electron microscopy (SEM) has been used for the microstructural investigation. Detailed dielectric properties of the compounds have been studied as a function of frequency and temperature. The variations of dielectric constant (ε'_r) with temperature show that the compounds undergo a diffuse type ferro-paraelectric phase transition. The dielectric constant is found to increase with the increasing sintering temperature and duration. In all the samples, the variation of dielectric loss (tan δ) with temperature is observed to be almost constant initially but it increases as temperature is increased and a peak is observed only when the material is sintered at higher temperature for longer duration. The frequency dependence of dielectric constant and loss shows a decreasing trend up to nearly 10 kHz and beyond this frequency there is almost no variation. Also, the diffusivities of the samples have been calculated and it is found to increase with increasing sintering temperature and duration.

P. Ganguly (✉) · A. K. Jha · K. L. Deori
Thin Films & Materials Science Laboratory,
Department of Applied Physics, Delhi College of Engineering,
Delhi 110042, India
e-mail: gangulyprasun@yahoo.co.in

A. K. Jha
e-mail: dr_jha_ak@yahoo.co.in

1 Introduction

Since the discovery of ferroelctricity in BaTiO$_3$ [1], large number of new ferroelectric materials have been discovered having significant industrial and commercial applications. Materials in different structural groups like perovskite, tungsten–bronze (TB), spinel, pyrochlore are now well known [2–7]. Some niobates and tantalates with TB structure have attracted attention because of their interesting ferroelectric, pyroelectric, piezoelectric and nonlinear optical properties [8–14]. The TB-type structure consists of a complex array of distorted BO$_6$ octahedra sharing corners in such a way that three different types of interstices (A, B and C) are available for cation occupation in the general formula $[(A_1)_4(A_2)_2(C)_4][(B_1)_2(B_2)_8]O_{30}$ [15]. In this formula, A$_1$ and A$_2$ sites are usually filled by divalent or trivalent cations, B$_1$ and B$_2$ sites by tetravalent or pentavalent cations and C site being small, often remains empty giving the general formula A$_6$B$_{10}$O$_{30}$ for the tungsten–bronze structure. In this family, researchers have shown interest in Ba$_2$Na$_3$RNb$_{10}$O$_{30}$ (R=La, Y, Gd, Eu and Dy) [16], K$_2$LaNb$_5$O$_{15}$ [17], Ba$_4$NaNb$_{10}$O$_{30}$ [18], Ba$_5$SmTi$_3$Nb$_7$O$_{30}$ [19] compounds. However, to the best of our knowledge, not much work has been reported on Ba$_5$SmTi$_3$Nb$_7$O$_{30}$ compound by systematically varying the sintering condition. In this work, we have systematically studied the effect of sintering temperature and duration on the structure and properties of Ba$_5$SmTi$_3$Nb$_7$O$_{30}$.

2 Experimental

The polycrystalline samples of Ba$_5$SmTi$_3$Nb$_7$O$_{30}$ (BSTN) were prepared by solid-state reaction technique by taking high purity BaCO$_3$, TiO$_2$, Nb$_2$O$_5$ (all from M/s Aldrich, USA) and Sm$_2$O$_3$ (M/s Alfa Aesar, USA) in their
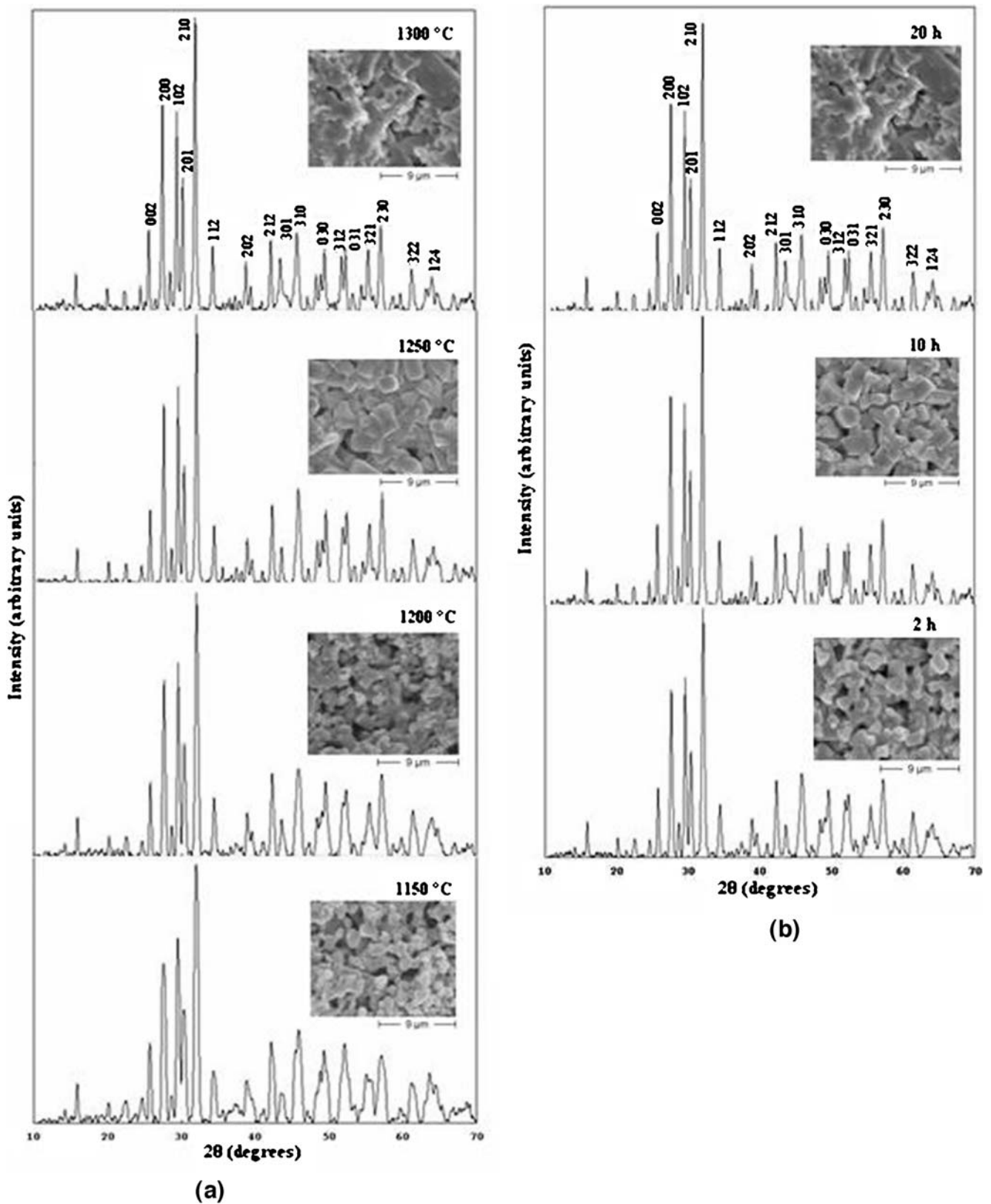
Fig. 1 XRD patterns of Ba₅SmTi₃Nb₇O₃₀ sintered at (**a**) different temperatures for 20 h and (**b**) different durations at 1300°C. In inset the respective SEM micrographs of the samples are shown

Table 1 Lattice parameters, relative density, average grain size, dielectric properties (at 100 kHz) and diffusivity of $Ba_5SmTi_3Nb_7O_{30}$ synthesized at various sintering conditions.

| Sintering Conditions	a (Å)	b (Å)	c (Å)	Relative Density (%)	Average Grain Size (μm)	$\varepsilon'_{R.T.}$	ε'_{max}	T_c (°C)	γ
1150°C; 20 h	6.5198	5.6101	6.9338	62.41	1.4	64.9838	86.3004	210	1.34
1200°C; 20 h	6.5398	5.5728	6.9253	65.66	1.8	88.3513	132.3420	180	1.47
1250°C; 20 h	6.5374	5.5397	6.9001	74.84	2.6	154.0528	232.2804	170	1.73
1300°C; 20 h	6.4050	5.5566	6.8005	90.23	4.2	259.1363	416.0325	165	1.95
1300°C; 10 h	6.4106	5.5595	6.8112	80.34	2.2	193.5925	303.1267	170	1.71
1300°C; 2 h	6.3858	5.5435	6.7648	70.14	1.6	136.4142	207.0189	185	1.45

stoichiometric proportions. The materials were thoroughly ground in an agate mortar and passed through sieve of appropriate size. This powder mixture was then calcined at 1100°C for 20 h in an alumina crucible. The calcined mixture were ground and admixed with 4–5 wt.% polyvinyl

alcohol (PVA) as a binder and then pressed at ~300 MPa into disk shaped pellets. These pellets were then sintered at different sintering conditions. One set of pellets were sintered at temperatures from 1150 to 1300°C at an interval of 50°C for 20 h and another set of pellets were sintered at 1300°C for 2 h, 10 h and 20 h.

X-ray diffractograms of all the sintered pellets were recorded using Philips (X'Pert Model) diffractometer in the
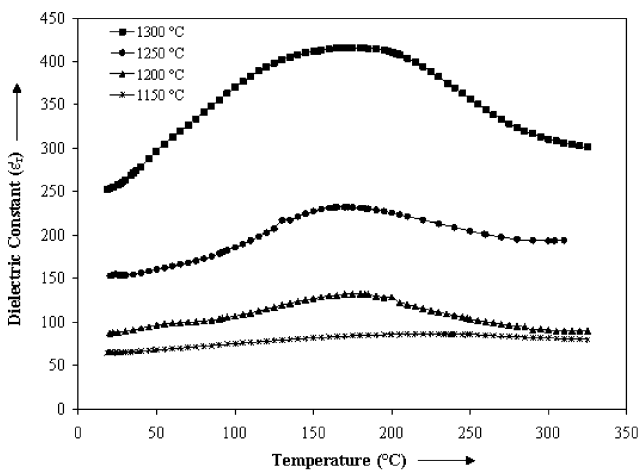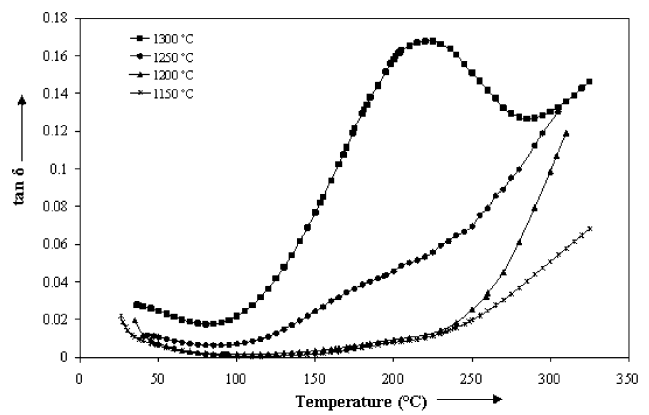

(a)
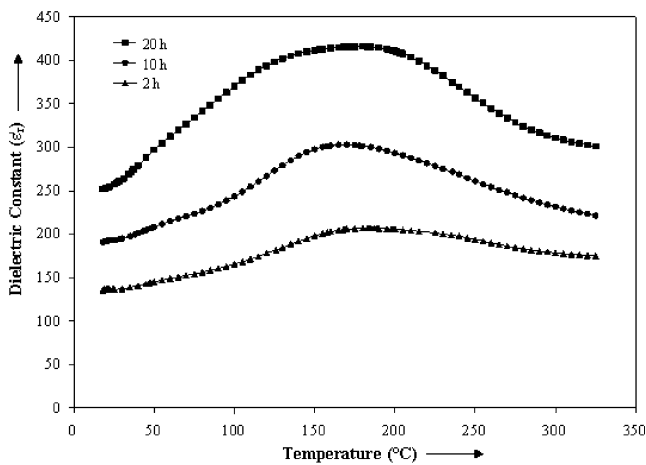
(b)

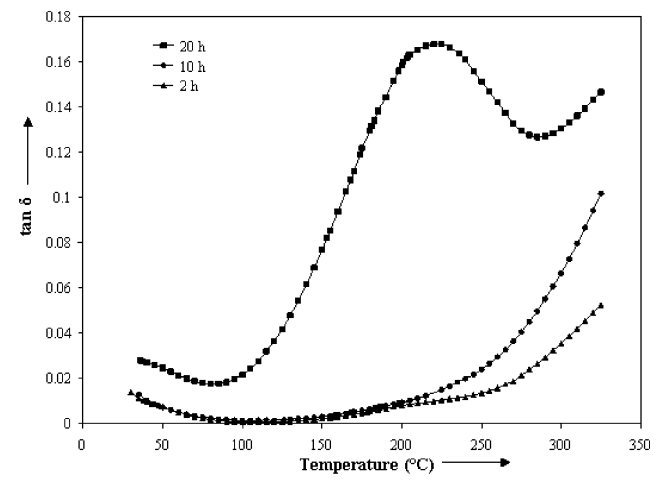**Fig. 2** Variation of dielectric constant with temperature at different (**a**) sintering temperature and (**b**) sintering time at 100 kHz

(a)

(b)

Fig. 3 Variation of dielectric loss (tan δ) with temperature at different (**a**) sintering temperature and (**b**) sintering time at 100 kHz
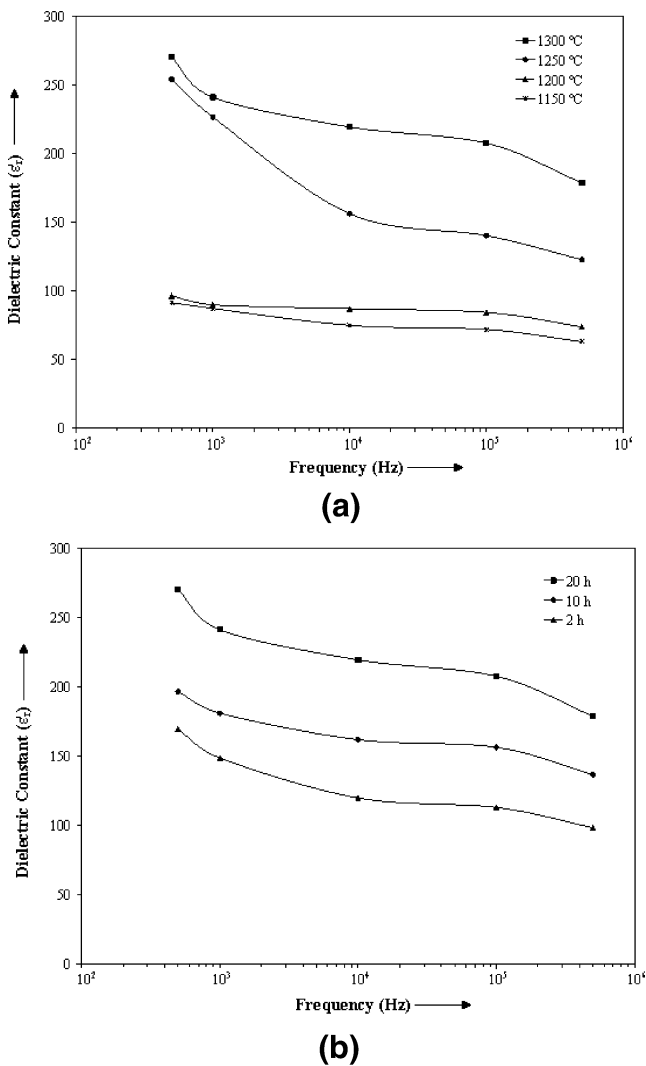
Fig. 4 Variation of dielectric constant (ε_r') with frequency at different (**a**) sintering temperature and (**b**) sintering time at room temperature
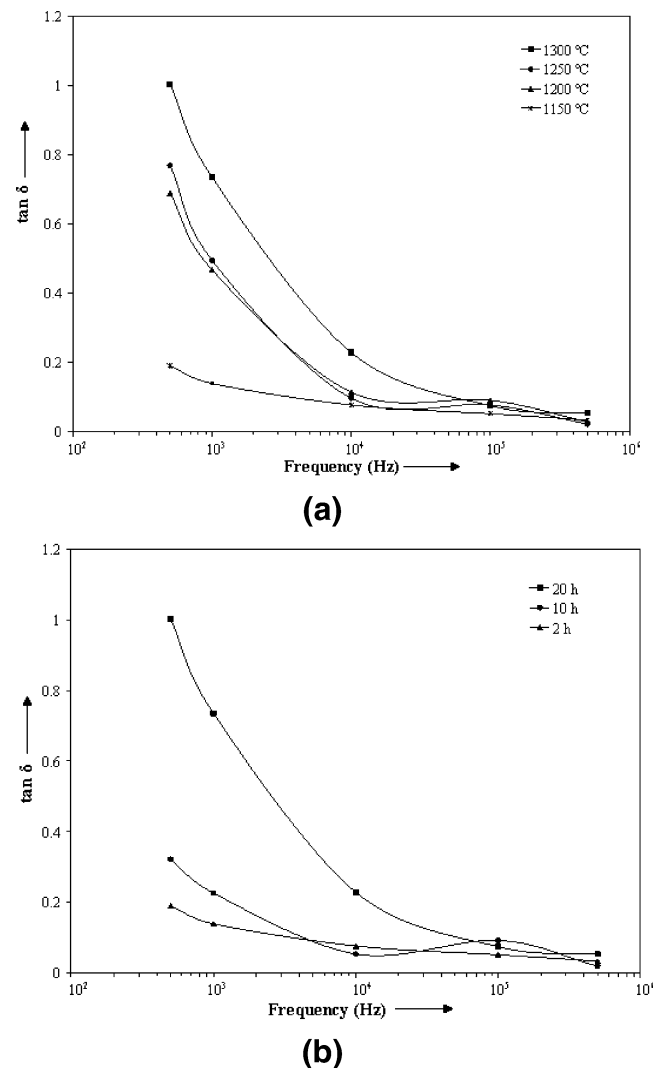

Fig. 5 Variation of dielectric loss (tan δ) with frequency at different (**a**) sintering temperature and (**b**) sintering time at room temperature

range $10° \leq 2\theta \leq 70°$ with CuK_{α} radiation (λ=1.5405 Å). The densities of the sintered pellets were measured using Archimedes principle in a laboratory made set-up with ethylene glycol. The microstructural study of the samples was carried out using Scanning Electron Microscope (Jeol, JSM—840), operated at 20 kV. The sintered pellets were polished and coated with silver paste on both sides to act as electrodes and cured at 325°C for 1 h. The dielectric measurements were carried out using HP 4284A LCR meter operating at oscillation amplitude of 1 V.

3 Results and discussion

Figure 1(a) and (b) shows the X-ray diffraction patterns of all the studied samples which reveal the formation of single-phase compounds. However, some peaks of the samples with lower sintering temperature are merged indicating incomplete growth of the phase. The lattice parameters of the samples were calculated (Table 1) using the observed interplanar spacing d-values from the diffractograms and refined using the least square refinement method by a computer program package PowderX [20]. The observed decrease in lattice parameters on increase in sintering temperature is possibly due to increased formation of oxygen vacancies discussed later in the text. The peaks have been indexed using the observed d and the calculated lattice parameters. From these results, it is found that BSTN samples sintered at above mentioned sintering conditions have an orthorhombic crystal with a TB-type structure.

The values of the relative density of the samples are given in Table 1. It is observed that relative density increases as the sintering temperature and time increases. This is possibly due to decrease in the porosity and increase in the grain size of
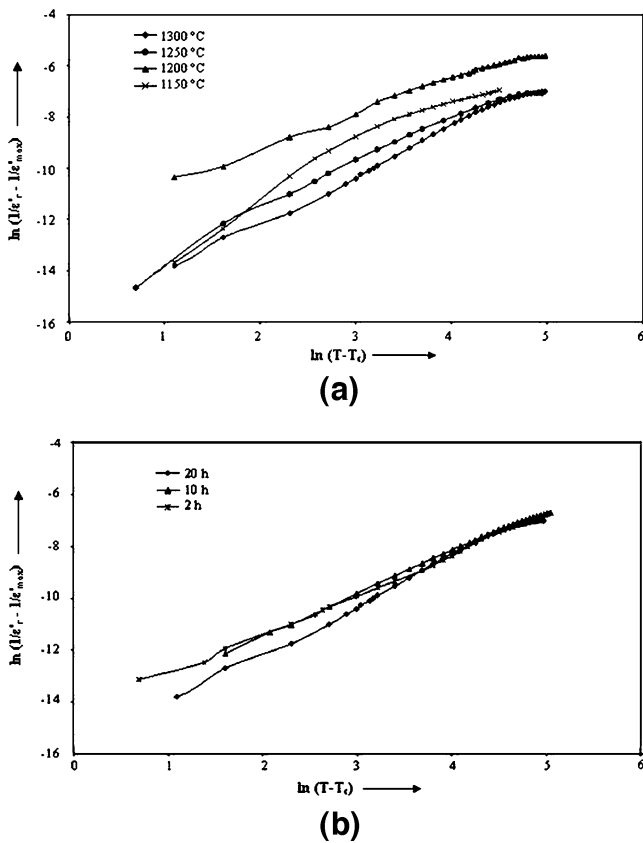
Fig. 6 Variation of $\ln\left(1/\varepsilon'_r - 1/\varepsilon'_{max}\right)$ with $\ln(T-T_c)$ as a function of (**a**) sintering temperature and (**b**) sintering duration

the specimens as seen in SEM micrographs (Fig. 1(a) and (b) inset) with increase in the sintering temperature and time, also given in Table 1.

The dielectric constant $\left(\varepsilon'_r\right)$ and dielectric loss (tan δ) of the studied samples sintered at various sintering temperatures were measured from room temperature to 325°C at 100 kHz frequency. The maximum dielectric constant $\left(\varepsilon'_{max}\right)$ and room temperature dielectric constant $\left(\varepsilon'_{R.T}\right)$ value of all the samples are given in Table 1 with their curie temperatures (T_c). In all the samples, a diffuse type of ferro-paraelectric phase transition is observed. Figure 2(a) and (b) shows the temperature variation of dielectric constant at 100 kHz for different sintering temperature and time. It is found that ε'_r increases as sintering temperature and duration of the BSTN samples increases. The increase in ε'_r can be understood by the increase in the grain size with increase in sintering temperature and time (Table 1). The higher sintering temperature for longer duration enhances the average grain size, making the domain wall motion easier resulting in an increased dielectric constant [21]. Also, it is known that these TB structured compounds are expected to lose oxygen during sintering at high temperature [22, 23] as per the reaction which can be represented by Kröger and Vink notation [24]:

$$O_o \rightarrow \frac{1}{2} O_2 \uparrow + V_o^{\bullet\bullet} + 2e^-$$
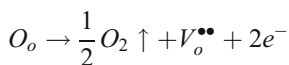
where $V_o^{\bullet\bullet}$ denotes oxygen vacancies. The defects such as oxygen vacancies $V_o^{\bullet\bullet}$, act as space charge. So as we increase the sintering temperature and duration in this material more and more oxygen vacancies are created. The increase in ε'_r value is known to be related to the oxygen ions or oxygen vacancies created during sintering [25]. This could be another possible cause for the increase in ε'_r as sintering temperature and duration of the BSTN samples increases.

Figure 3(a) and (b) depicts the temperature variation of dielectric loss at 100 kHz for different sintering conditions. It is observed that the loss increases with temperature. The loss is found to be higher in the sample which is sintered at higher sintering temperature for longer duration. The source of dielectric loss in insulating ceramics is space charge polarization and/or domain wall relaxation [26]. From the above discussion it is reasonable to believe that the space charge, in the form of oxygen vacancies, is primarily responsible for an appreciable increase in dielectric loss in the samples sintered at higher sintering temperature for longer durations. Also the loss increases with increase in temperature as the oxygen vacancy induced polarization becomes dominant at high temperatures [27]. Unlike other samples, a peak is observed in the tan δ versus temperature curve of the specimen sintered at 1300°C for 20 h. This could be the relaxation peak whose formation is attributed to the oxygen vacancies [28, 29] which are present in large concentration in this highly sintered sample of BSTN.

Figure 4(a) and (b) shows the frequency variation of ε'_r over the range 500 Hz to 500 kHz at room temperature of the studied samples. It is observed that ε'_r decreases steadily for samples sintered at 1250°C and 1300°C (for all durations) as the frequency increases from 500 Hz to 10 kHz and remains almost constant at frequencies above 10 kHz. However, the samples sintered at 1150°C and 1200°C, show no appreciable variation in ε'_r values in the entire frequency range. The dielectric constant of a material has four polarization contributions: electronic, ionic, dipolar and space charge [30]. In the present work, contribution from the dipolar polarization is not expected as the applied electric field of about 6 V/cm is too small to alter the orientation of the dipoles. Response frequencies for electronic and ionic polarizations are $\sim 10^{16}$ and 10^{13} Hz, respectively; and at frequencies above 10 kHz, contribution from space charge polarization is not expected [30]. As discussed above, as we increase the sintering temperature and time in the BSTN samples, more and more oxygen vacancies are generated. The defects such as oxygen vacancies, $V_o^{\bullet\bullet}$, acting as space charge play an important role in the polarization which becomes dominant at lower frequencies [31, 32]. The high value of ε'_r for low frequencies in case of samples sintered at higher temperatures (1250–1300°C) can thus be attributed to the presence of such space charges. Moreover, higher relative density

and larger grains size supports the observation of high ε'_r value in the samples sintered at higher temperatures (1250–1300°C). The small amount of oxygen vacancies in the samples sintered at lower temperature (1150–1200°C) results in negligible variation of ε'_r value with frequency.

Figure 5(a) and (b) shows the variation of tan δ with frequency at room temperature. It also decreases sharply upto 10 kHz for all the samples and beyond this it is almost independent of frequency. This can also be understood in terms of space charge as the source of dielectric loss in these materials is space charge polarization [26].

In all the samples, broad peak in dielectric constant vs. temperature curve is observed. The broadening of the dielectric peaks may be attributed to the occurrence of more disordering in the system on increasing sintering temperature and time. The degree of disorderness or the diffusivity constant (γ) has been calculated using the formula [33]

$$\ln\left(1/\varepsilon'_r - 1/\varepsilon'_{\max}\right) = \gamma \ln(T - T_c) + \text{constant}$$

The value of γ for all the samples at 100 kHz obtained from the slope of the curve $\ln\left(1/\varepsilon'_r - 1/\varepsilon'_{\max}\right)$ versus ln $(T–T_c)$, as shown in Fig. 6(a) and (b), has been found to be between 1 (obeying Curie-Weiss law) and 2 (for completely disordered system) (Table 1). It is found to increase with sintering temperature and duration indicating increase in disorderness in the system with increase in sintering temperature and time. This could be due to the defects (here oxygen vacancy) induced disorderness [34] which increases with increase in sintering temperature and duration.

4 Conclusions

For all sintering conditions undertaken in the present work, BSTN shows an orthorhombic crystal system with a TB-type structure. The density and the average grain size increases with increase in sintering temperature and time. The dielectric constant $\left(\varepsilon'_r\right)$ as well as dielectric loss (tan δ) increases significantly by increasing sintering temperature and time. However, a peak in the dielectric loss versus temperature curve has been observed only when the material is sintered at higher temperature for longer duration. The disorderness in the system is found to increase as the sintering temperature and duration is increased.

References

1. B.K. Wul, L.M. Goldman, C.R. Acad. Sci. URSS **46**, 133(1945)
2. I. Coondoo, A.K. Jha, S.K. Agarwal, N.C. Soni, J. Electroceram **16**, 393(2006)
3. I. Coondoo, A.K. Jha, S.K. Agarwal, J. Eur. Cer. Soc **27**, 253(2007)
4. V. Shrivastava, A.K. Jha, R.G. Menditta, Solid State Comm **133**, 125(2005)
5. C.F.G. Stenger, A.J. Burggraaf, J. Phys. Chem. Solids **41**, 17(1980)
6. C.F.G. Stenger, A.J. Burggraaf, J. Phys. Chem. Solids **41**, 25(1980)
7. K.S. Singh, R. Sati, R.N.P. Choudhary, J. Mater. Sci. Lett **11**, 788 (1992)
8. R.R. Neurgaonkar, W.F. Hall, J.R. Oliver, W.W. Ho, W.K. Cory, Ferroelectrics **87**, 167(1998)
9. R.R. Neurgaonkar, J.G. Nelson, J.R. Oliver, Mater. Res. Bull **25**, 959(1990)
10. R.R. Neurgaonkar, J.G. Nelson, J.R. Oliver, Mater. Res. Bull **27**, 677(1992)
11. N. Wakiya, J.K. Wang, A. Saiki, K. Shinozaki, N. Mizutani, J. Eur. Ceram. Soc **19**, 1071(1999)
12. Z.X. Cheng, S.J. Zhang, G.Y. Zhou, J.H. Liu, J.R. Han, H.C. Chen, Mater. Res. Bull **35**, 1107(2000)
13. Y.K. Hwang, Y.U. Kwon, Mater. Res. Bull **32**, 1495(1997)
14. B. Tribotte, J.M. Haussonne, G. Desgardin, J. Eur. Ceram. Soc **19**, 1105(1999)
15. P.B. Jasmieson, S.C. Abrahams, L. Bernstein, J. Chem. Phys **48**, 5048(1965)
16. J.L. Mukherjee, J. Solid State Chem **24**, 163(1978)
17. H. Iwaski, Mater. Res. Bull **6**, 251(1971)
18. K.V. Masuno, J. Phys. Soc. Jpn **19**, 323(1964)
19. S.R. Shannigrahi, R.N.P. Choudhary, A. Kumar, H.N. Acharya, J. Phys. Chem. Solids **59**, 737(1998)
20. C. Dong, J. Appl. Cryst **32**, 838(1999)
21. H.T. Martirena, J.C. Burfoot, J. Phys. C: Solid State Phys **7**, 3162 (1976)
22. C.K. Suman, K. Prasad, R.N.P. Choudhary, J. Mat. Sci **41**, 369 (2006)
23. C.K. Suman, K. Prasad, R.N.P. Choudhary, Mat. Chem. & Phys **82**, 140(2003)
24. F.A. Kröger, H.J. Vink, Solid State Phys **3**, 307(1956)
25. P. Goel, K.L. Yadav, Mat. Lett **60**, 3183(2006)
26. I.S. Zheludev, *Physics of Crystalline Dielectrics, Vol I: Crystallography & Spontaneous Polarization* (Plenum, New York (1971)
27. T. Friessnegg, S. Aggarwal, R. Ramesh, B. Nielsen, E.H. Poindexter, D.J. Keeble, Appl. Phys. Lett **77**, 127(2000)
28. W.P. Lu, X.Y. Mao, X.B. Chen, J. Appl. Phys **95**, 1973(2004)
29. W.P. Lu, J. Zhu, H. Sun, X.B. Chen, J. Mat. Res **20**, 971(2005)
30. R.C. Buchanan, *Ceramic Materials for Electronics: Processing, Properties and Applications* (Marcel Dekker, New York (1986), p. 38
31. Y. Noguchi, M. Miyayama, Appl. Phys. Lett **78**, 1903(2001)
32. A. Chen, Y. Zhi, L.E. Cross, Phys. Rev. B **62**, 228(2000)
33. S.M. Pilgrim, A.E. Sutherland, S.R. Winzer, J. Am. Ceram. Soc **73**, 3122(1990)
34. V. Raghavan, *Materials Science and Engineering* (Prentice-Hall of India, New Delhi (2004), p. 194